Electronic Supplementary Material (ESI) for Journal of Materials Chemistry B.

Supporting Information for

In situ Formation of J-Aggregate in Tumor Microenvironment Using Acidity-Responsive Polypeptide Nanoparticles Encapsulating Galactose Conjugated BODIPY Dye for NIR-II Phototheranostics

Huiping Dang, Dalong Yin, Youliang Tian, Quan Cheng, Changchang Teng, Yixuan Xu, Lifeng Yan *

Department of Hepatobiliary Surgery, The First Affiliated Hospital, Division of Life Sciences and Medicine, and Department of Chemical Physics, University of Science and Technology of China, Hefei, 230026, China.

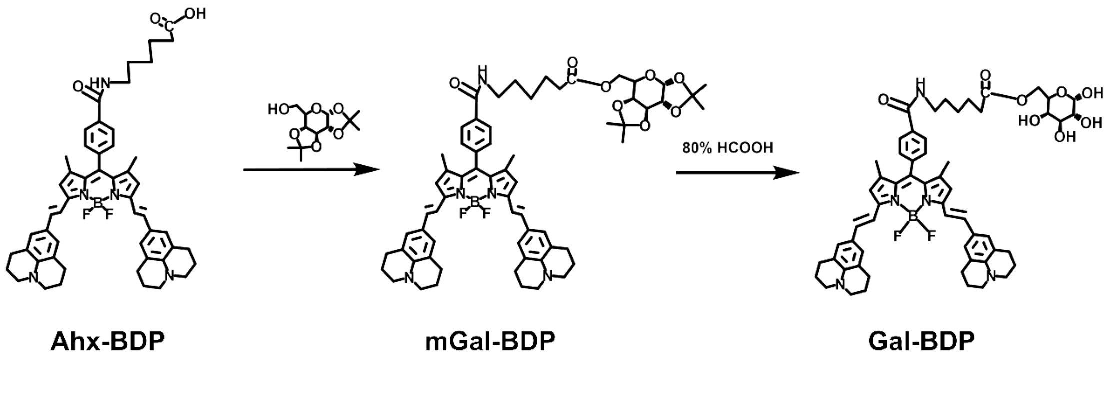

Figure S1. Synthesis of Gal-BDP.

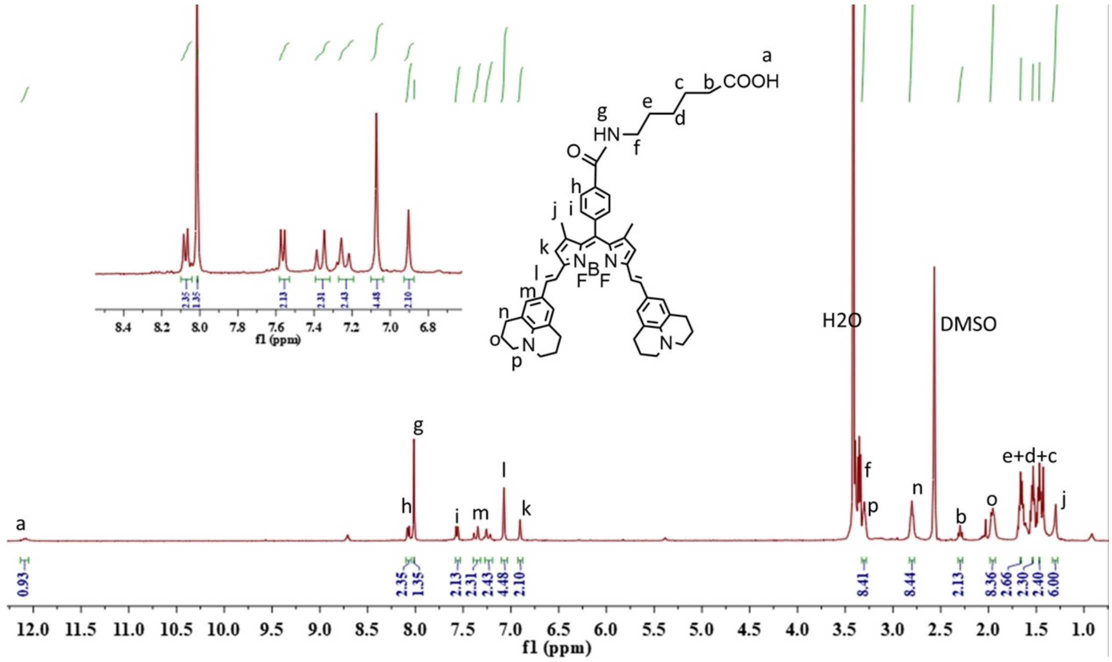

Figure S2. ^{1}H NMR spectrum of Ahx-BDP.

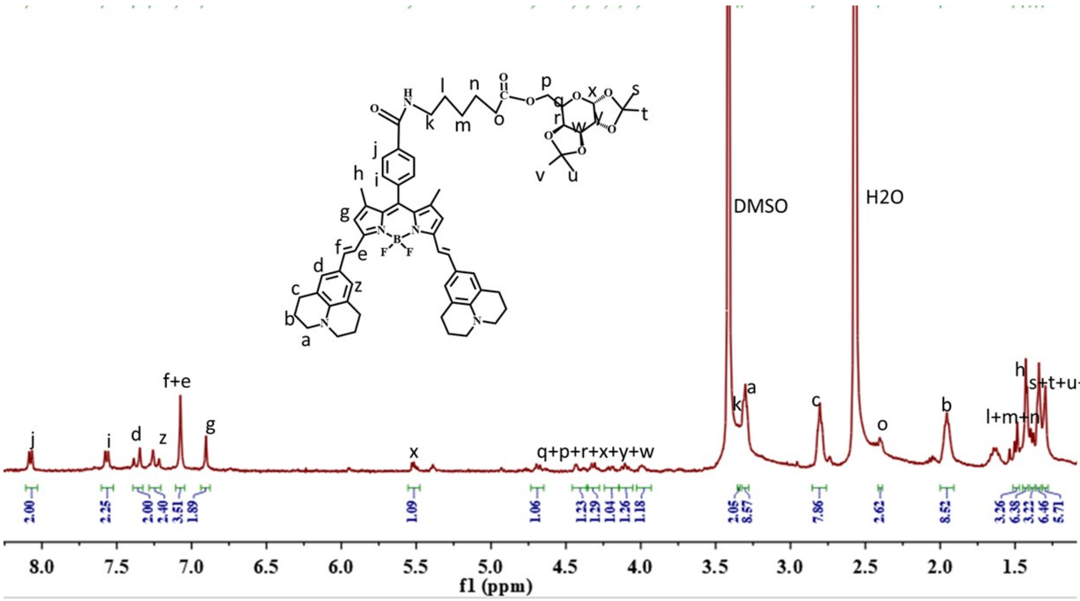

Figure S3. ^{1}H NMR spectrum of mGal-BDP.

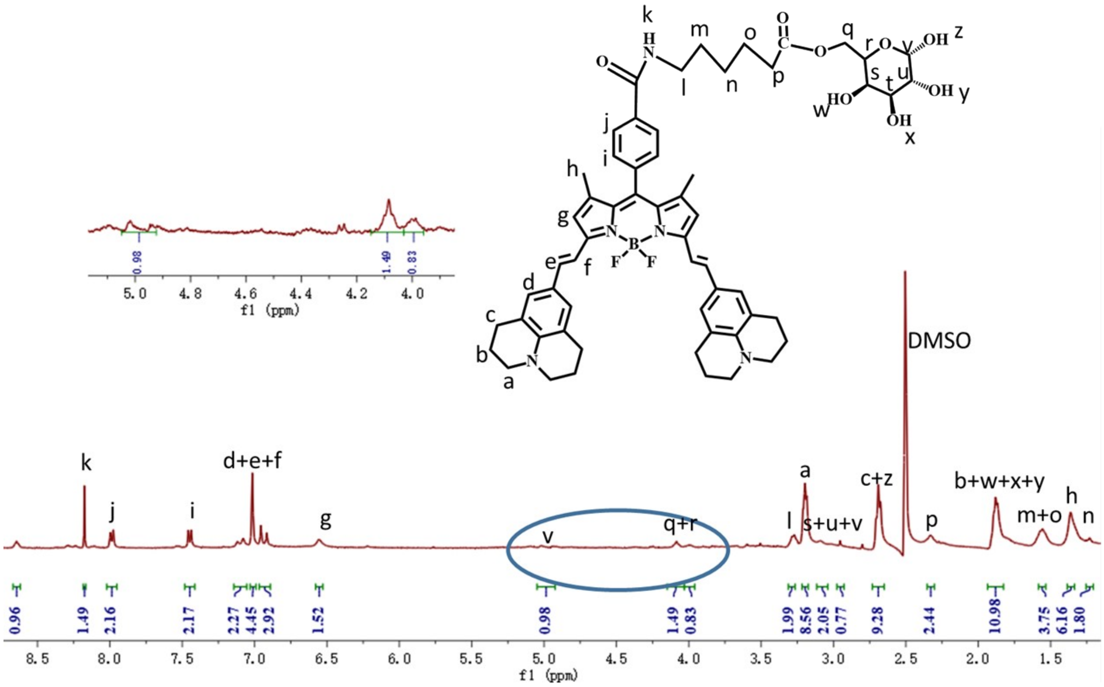

Figure S4. ^{1}H NMR spectrum of Gal-BDP.

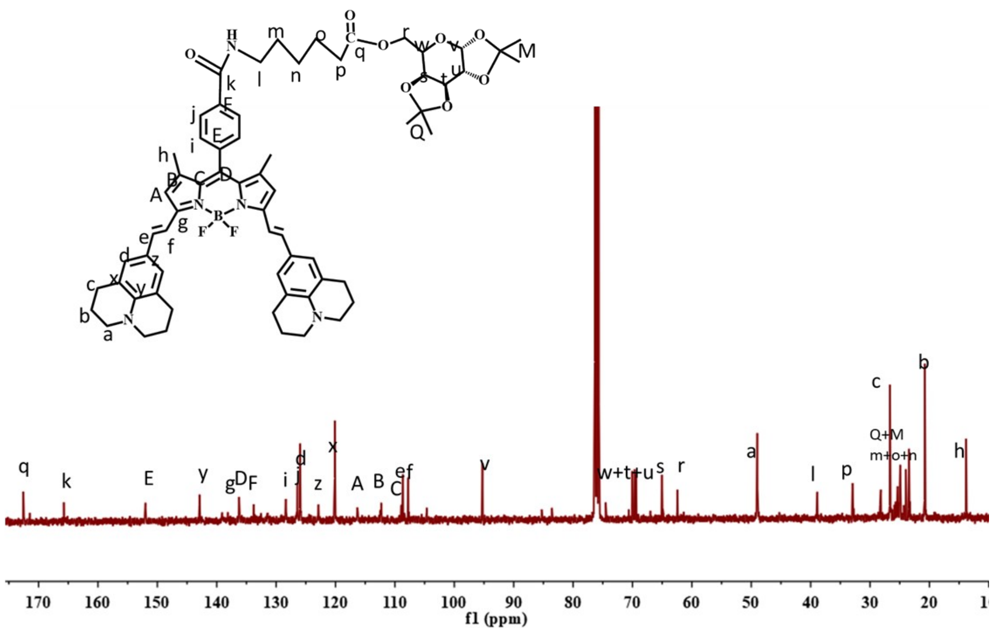

Figure S5. ^{13}C NMR spectrum of mGal-BDP.

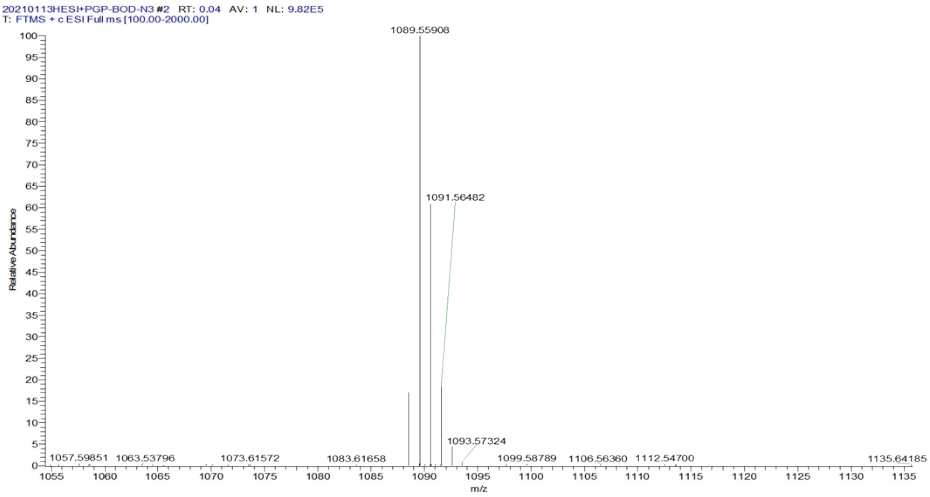

Figure S6. Mass spectra (ESI) of mGal-BDP.

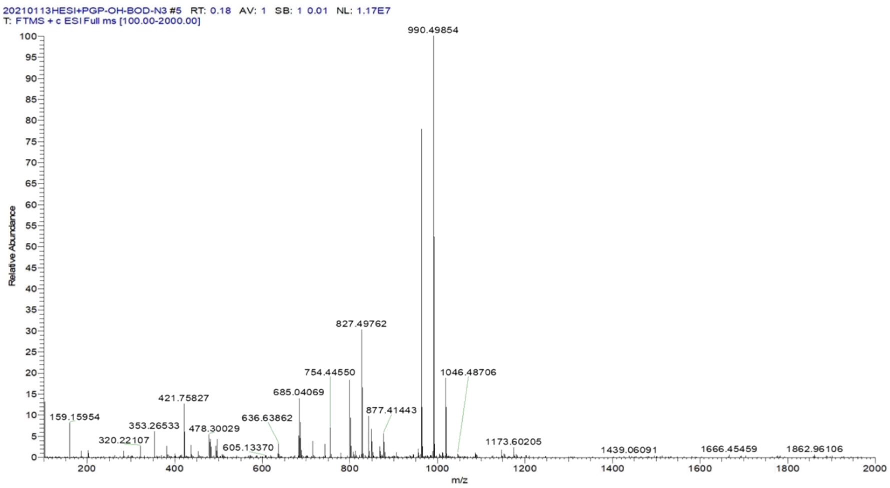

Figure S7. Mass spectra (ESI) of Gal-BDP.

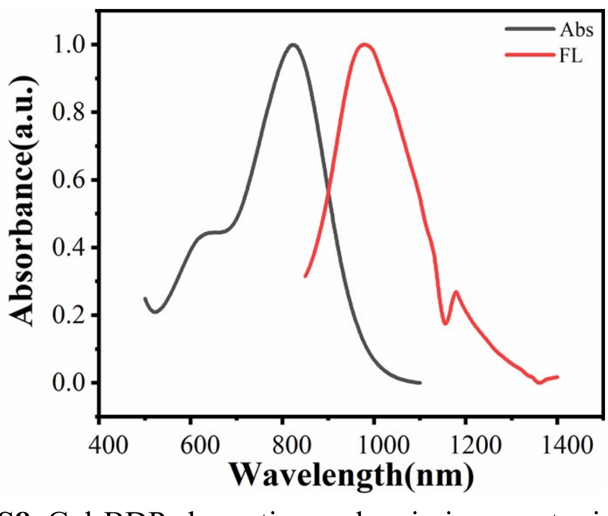

Figure S8. Gal-BDP absorption and emission spectra in DCM.

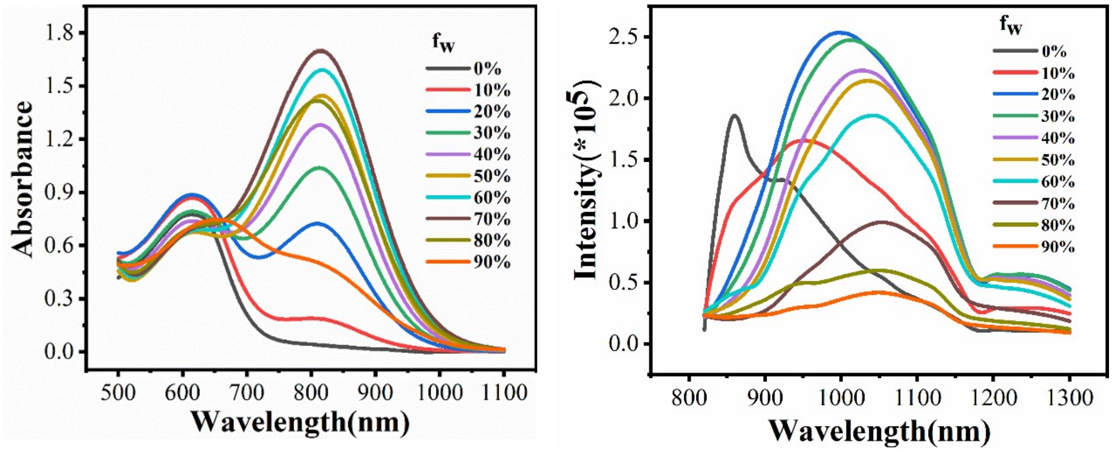

Figure S9. Gal-BDP absorption(left) and emission(right) spectra in in THF-H_2O.

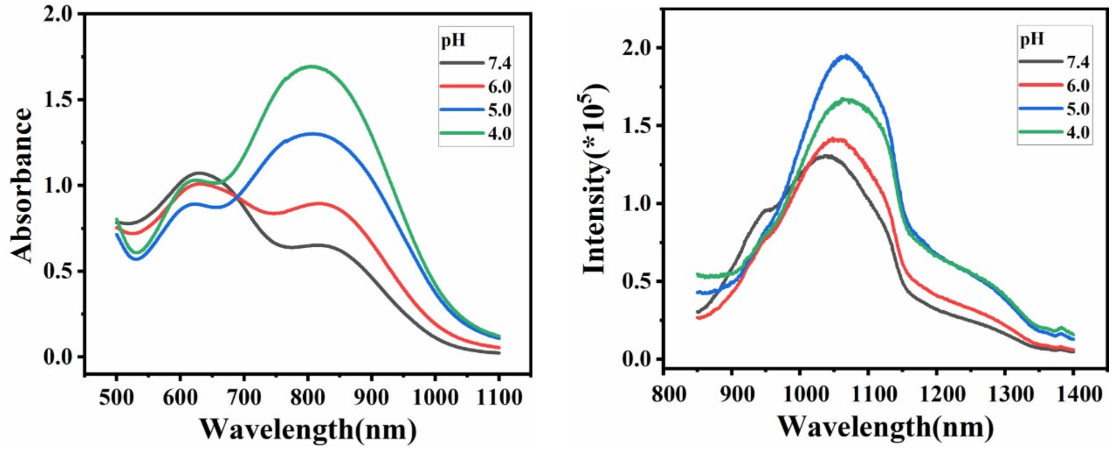

Figure S10. Changes of Gal-BDP absorption(left) and emission(right) spectra in different pH buffers.

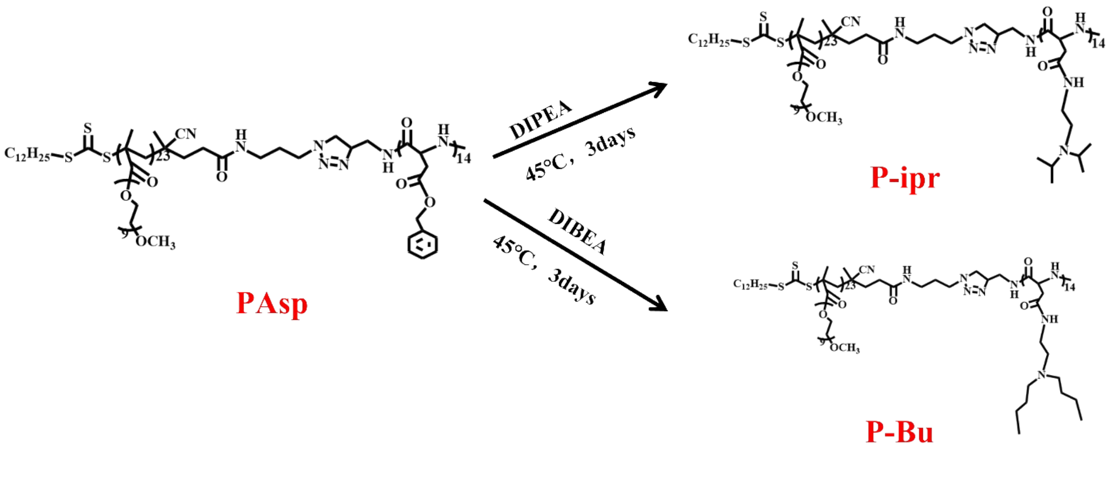

Figure S11. Polymer synthesis.

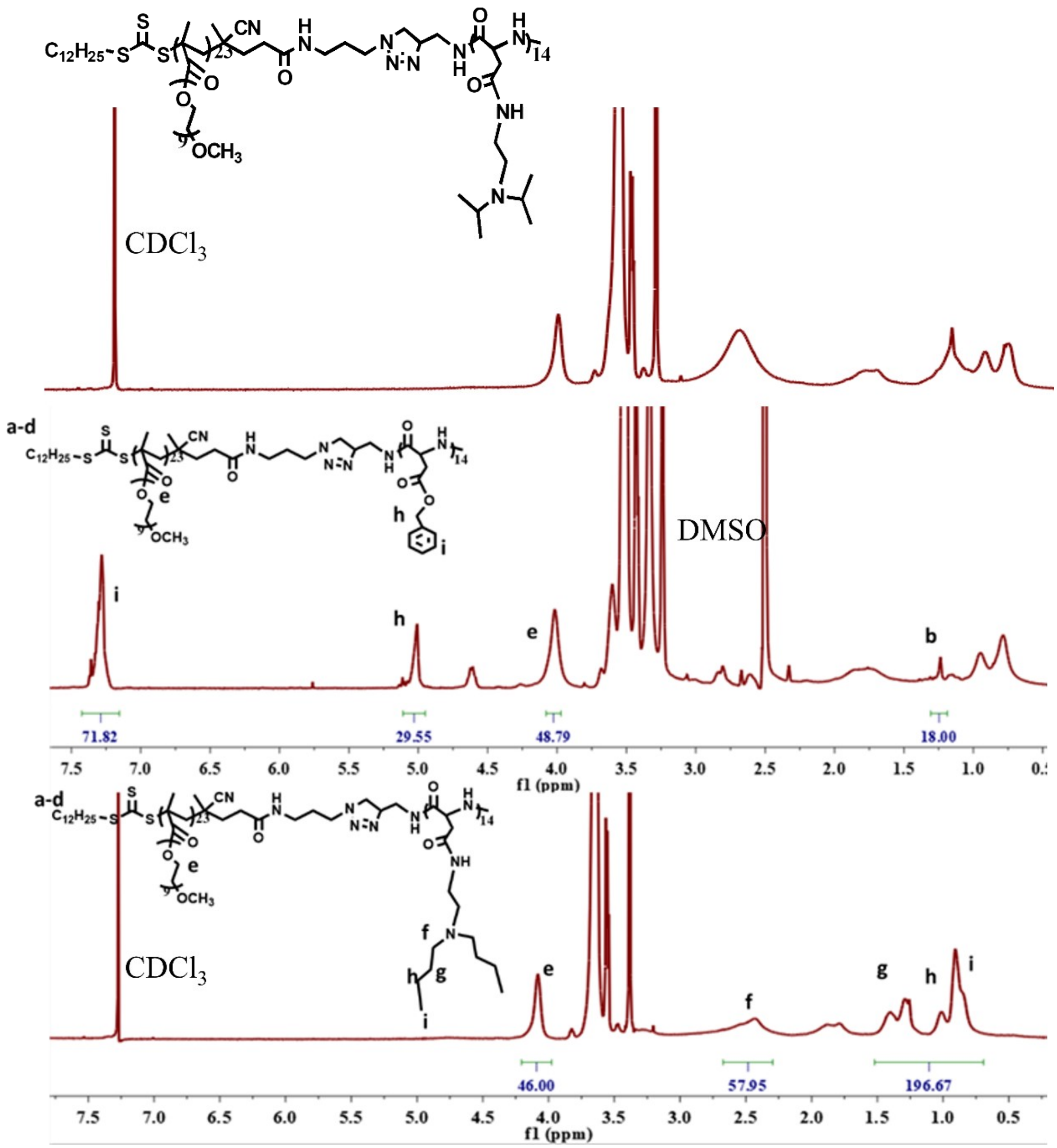

Figure S12. ¹H NMR spectrum of polymer.

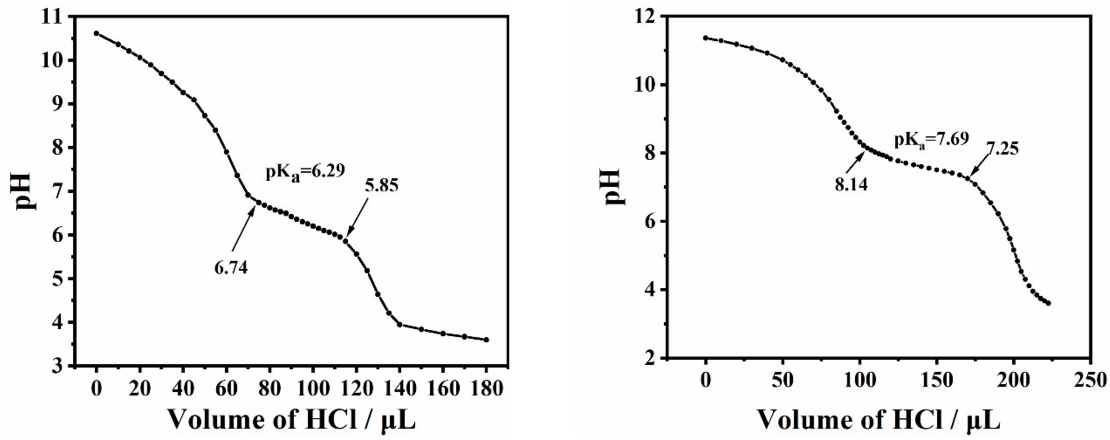

Figure S13. Titration curves of pH-sensitive P-ipr (left) and P-Bu (right) copolymers.

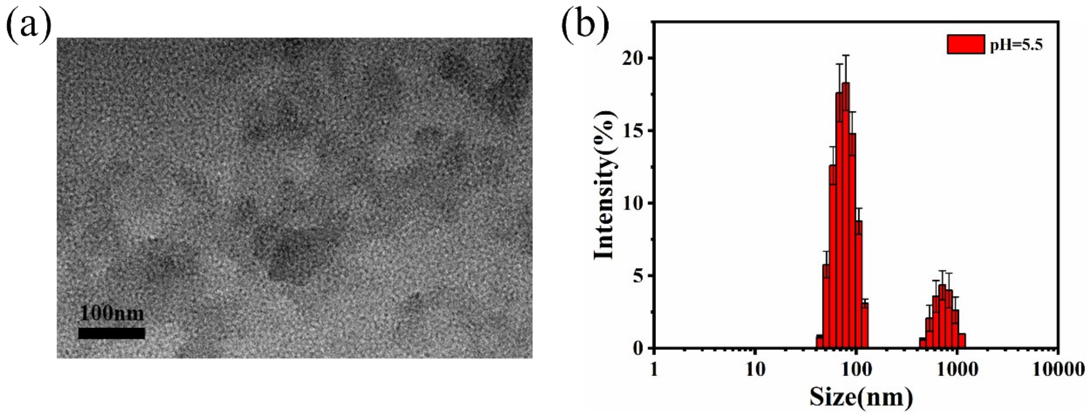

Figure S14. The TEM morphology(a) and DLS intensity distribution(b) of P-ipr@Gal NPs in pH = 5.5.

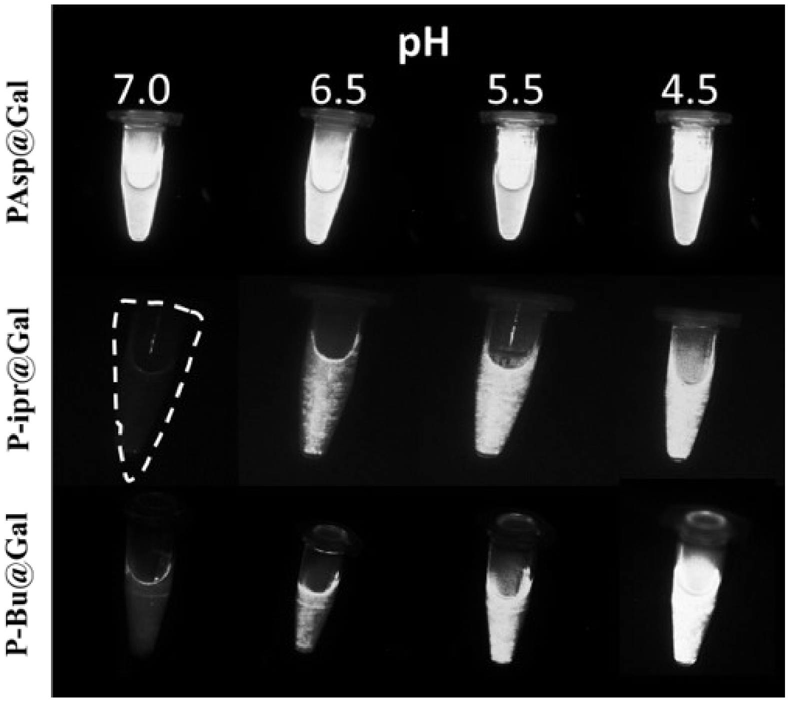

Figure S15. Fluorescence imaging of different nanoparticle solutions in different pH buffers.

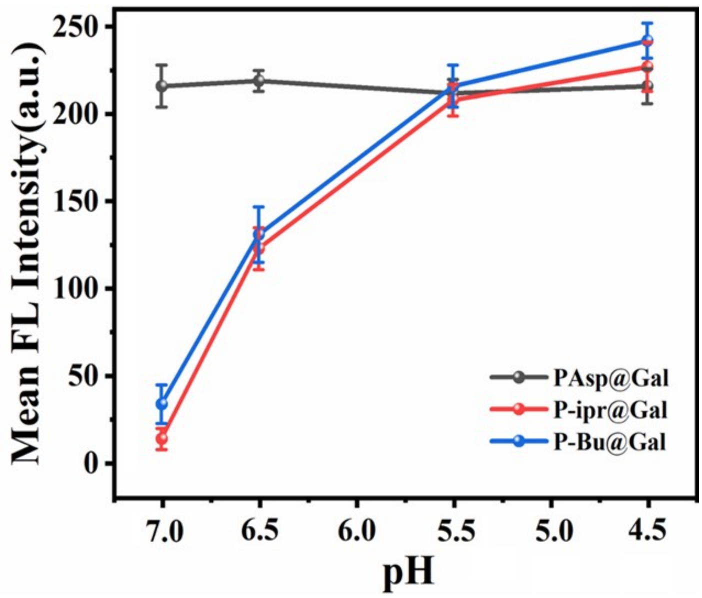

Figure S16. The quantitative variation of fluorescence brightness with pH.

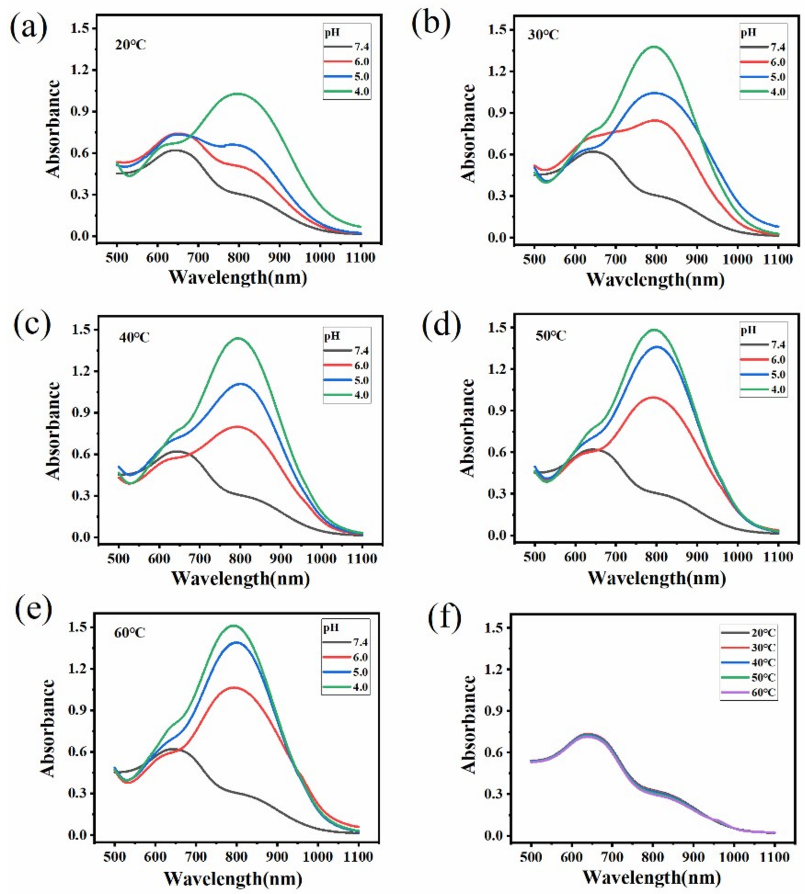

Figure S17. The absorption spectra changes in different pH buffers at 20°C (a), 30°C(b), 40°C (c), 50°C(d), 60°C(e), respectively, and the thermal stability(f) of P-ipr@Gal.

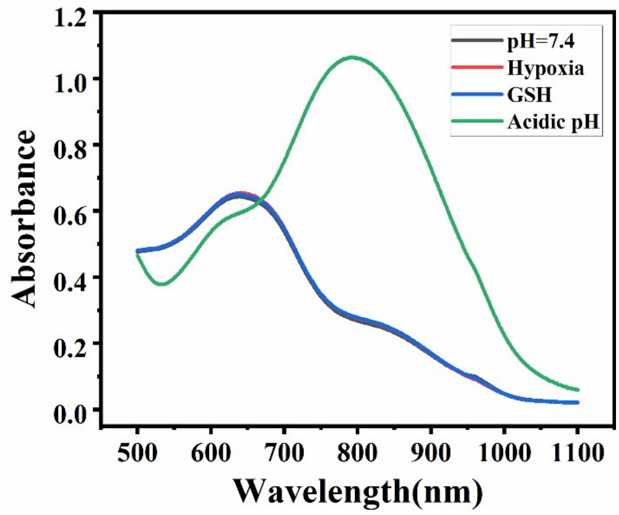

Figure S18. The absorption spectra of P-ipr@Gal nanoparticle in tumor microenvironment conditions.

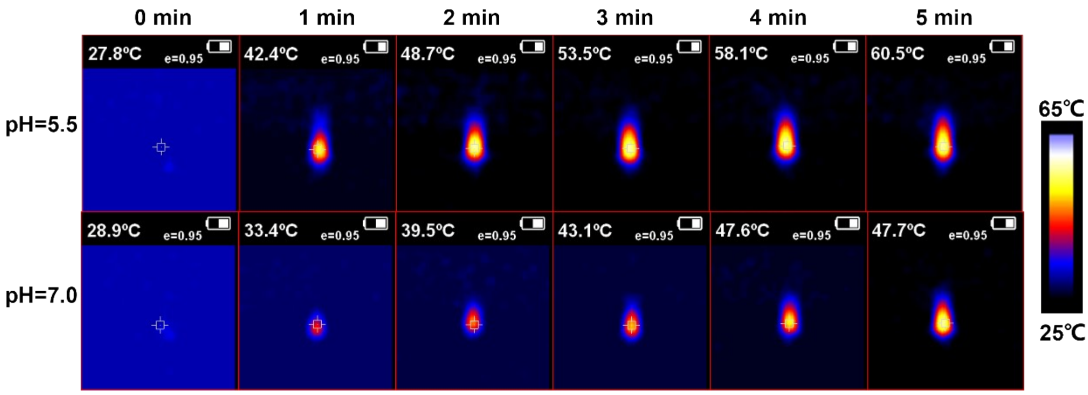

Figure S19. Infrared thermal images of P-ipr@Gal (30 ×10^{-6}M) during 5 minutes of irradiation by 808 nm laser (1 W cm^{-2}).

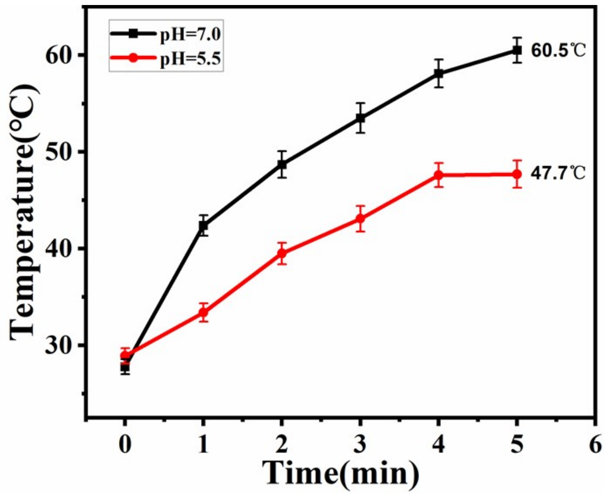

Figure S20. Corresponding temperature changes of P-ipr@Gal during the irradiation of 808 nm laser, the data are shown as mean ± SD (n = 3).

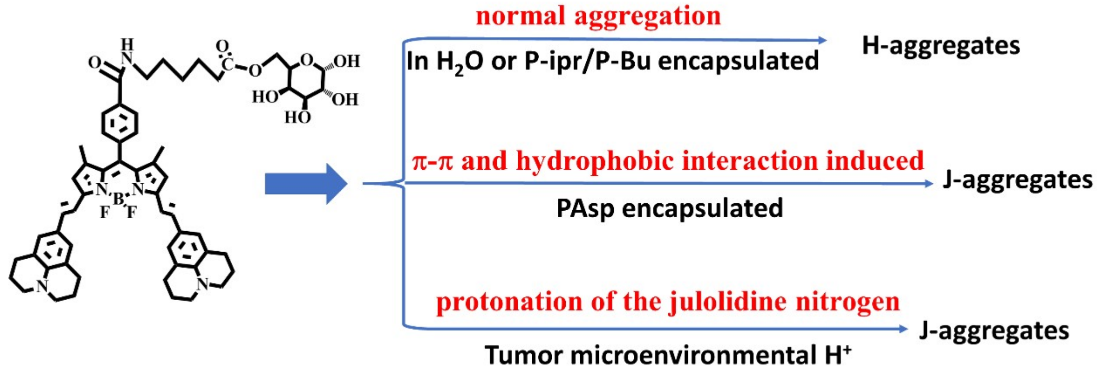

Figure S21. Aggregates of Gal-BDP under different environments.